Bcl-2–Modifying Factor Induces Renal Proximal Tubular Cell Apoptosis in Diabetic Mice

Bcl-2–Modifying Factor Induces Renal Proximal Tubular Cell Apoptosis in Diabetic Mice

Garnet J. Lau,[1] Nicolas Godin,[1] Hasna Maachi,[1] Chao-Sheng Lo,[1] Shyh-Jong Wu,[1] Jian-Xin Zhu,[1] Marie-Luise Brezniceanu,[1] Isabelle Chénier,[1] Joelle Fragasso-Marquis,[1] Jean-Baptiste Lattouf,[1] Jean Ethier,[1] Janos G. Filep,[2] Julie R. Ingelfinger,[3] Viji Nair,[4] Matthias Kretzler,[4] Clemens D. Cohen,[5] Shao-Ling Zhang,[1] and John S.D. Chan[1]

This study investigated the mechanisms underlying tubular apoptosis in diabetes by identifying proapoptotic genes that are differentially upregulated by reactive oxygen species in renal proximal tubular cells (RPTCs) in models of diabetes. Total RNAs isolated from renal proximal tubules (RPTs) of 20-week-old heterozygous *db/m+*, *db/db*, and *db/db* catalase (CAT)-transgenic (Tg) mice were used for DNA chip microarray analysis. Real-time quantitative PCR assays, immunohistochemistry, and mice rendered diabetic with streptozotocin were used to validate the proapoptotic gene expression in RPTs. Cultured rat RPTCs were used to confirm the apoptotic activity and regulation of proapoptotic gene expression. Additionally, studies in kidney tissues from patients with and without diabetes were used to confirm enhanced proapoptotic gene expression in RPTs. Bcl-2–modifying factor (Bmf) was differentially upregulated ($P < 0.01$) in RPTs of *db/db* mice compared with *db/m+* and *db/db* CAT-Tg mice and in RPTs of streptozotocin-induced diabetic mice in which insulin reversed this finding. In vitro, Bmf cDNA overexpression in rat RPTCs coimmunoprecipated with Bcl-2, enhanced caspase-3 activity, and promoted apoptosis. High glucose (25 mmol/L) induced Bmf mRNA expression in RPTCs, whereas rotenone, catalase, diphenylene iodinium, and apocynin decreased it. Knockdown of Bmf with small interfering RNA reduced high glucose–induced apoptosis in RPTCs. More important, enhanced Bmf expression was detected in RPTs of kidneys from patients with diabetes. These data demonstrate differential upregulation of Bmf in diabetic RPTs and suggest a potential role for Bmf in regulating RPTC apoptosis and tubular atrophy in diabetes. ***Diabetes*** **61:474–484, 2012**

Although the classic view of diabetic nephropathy (DN) has focused on events leading to glomerular dysfunction, the gradual decline of renal function in later stages of DN is invariably associated with tubulointerstitial fibrosis and tubular atrophy (1). Indeed, tubulointerstitial fibrosis and tubular atrophy appear to be better predictors of late-stage renal disease progression than glomerular pathology (2–5). For example, examination of nephrons from proteinuric diabetic patients shows that 71% of glomeruli display glomerulotubular junction abnormalities and 8–17% of glomeruli are atubular glomeruli (6,7).

The mechanisms underlying tubular atrophy are incompletely delineated. Studies have shown that high glucose (HG) concentrations are associated with increased reactive oxygen species (ROS) production, which inhibits proximal tubular function and induces apoptosis (8–10). Apoptosis has been detected in renal proximal tubular cells (RPTCs) of diabetic mice (11,12) and rats (13,14) as well as in RPTCs of diabetic patients (15–17), suggesting that tubular apoptosis may precede tubular atrophy in atubular glomeruli. Although the link between ROS and tubular apoptosis seems clear, little is known about the genes involved in HG-induced RPTC apoptosis or ROS generation.

We previously reported that HG enhances angiotensinogen (*Agt*) gene expression via ROS generation in rat RPTCs in vitro (18,19) and that in vivo overexpression of rat Agt in RPTCs induces hypertension, albuminuria, and RPTC apoptosis in diabetes (20). Conversely, we also reported that RPTC-selective overexpression of catalase (CAT) attenuates ROS generation, tubulointerstitial fibrosis, and tubular apoptosis as well as proapoptotic gene expression in diabetic mouse kidneys in vivo (21,22). These data suggest that ROS generation may be directly or indirectly responsible for RPTC apoptosis in diabetes.

We now report that Bcl-2–modifying factor (Bmf), a proapoptotic gene that we identified via DNA chip microarray analysis, is differentially upregulated in RPTCs of *db/db* mice; we also validated this observation by immunohistochemistry and real-time quantitative PCR (qPCR). We further show enhanced Bmf expression in the RPTCs of mice with streptozotocin (STZ)-induced diabetes as well as in the kidneys of patients with diabetes. Finally, we found that Bmf overexpression enhances RPTC apoptosis and that HG in vitro induces Bmf mRNA expression via ROS generation and transforming growth factor-β1 (TGF-β1) expression.

RESEARCH DESIGN AND METHODS

Chemicals and constructs. D-glucose, D-mannitol, diphenylene iodinium (DPI, an inhibitor of NADPH oxidase), rotenone (an inhibitor of mitochondrial electron transport chain complex I), apocynin (an inhibitor of NADPH oxidase), CAT, and monoclonal antibodies against β-actin were purchased from Sigma-Aldrich Canada Ltd. (Oakville, ON, Canada). Normal glucose (5 mmol/L), Dulbecco's Modified Eagle's Medium (DMEM), 100× penicillin/streptomycin, FBS, and the expression vector pcDNA 3.1 were purchased from InVitrogen, Inc. (Burlington, ON, Canada). The caspase-3 activity assay kit was purchased from BD Biosciences Pharmingen (Mississauga, ON, Canada). Anti-Bmf and anti–c-Myc polyclonal antibodies were purchased from Santa Cruz Biotechnology, Inc. (Santa Cruz, CA). Active human TGF-β1 was purchased from R&D Systems (Hornby, ON, Canada). Scrambled Silencer Negative Control # 1 small interfering RNA (siRNA) and siRNAs for TGF-β1 and Bmf were procured from Qiagen, Inc.

From the [1]Centre de recherche du Centre hospitalier de l'Université de Montréal (CRCHUM), Hôtel-Dieu Hospital, Université de Montréal, Montreal, Quebec, Canada; the [2]Research Centre, Maisonneuve-Rosemont Hospital, Montreal, Quebec, Canada; the [3]Pediatric Nephrology Unit, Massachusetts General Hospital, Harvard Medical School, Boston, Massachusetts; [4]Nephrology/Internal Medicine, Center for Computational Medicine and Bioinformatics, University of Michigan, Ann Arbor, Michigan; and the [5]Division of Nephrology, Institute of Physiology, University Hospital of Zurich, University of Zurich, Zurich, Switzerland.
Corresponding author: John S.D. Chan, john.chan@umontreal.ca.
Received 5 February 2011 and accepted 26 October 2011.
DOI: 10.2337/db11-0141
This article contains Supplementary Data online at http://diabetes.diabetesjournals.org/lookup/suppl/doi:10.2337/db11-0141/-/DC1.
G.J.L., N.G., and H.M. contributed equally to this study.
S.J.W. is currently affiliated with the Faculty of Biomedical Laboratory Science, Kaohsiung Medical University, Kaohsiung, Taiwan, Republic of China.

(Toronto, ON, Canada) and Ambion, Inc. (Austin, TX), respectively. Oligonucleotides were synthesized by InVitrogen, Inc. Restriction enzymes were purchased from InVitrogen, Inc. or Roche Biochemicals (Laval, QC, Canada).

CAT cDNA was a gift from Dr. Paul E. Epstein (University of Louisville, Louisville, KY). The plasmid pKAP2 containing the kidney-specific androgen-regulated protein (KAP) promoter responsive to testosterone stimulation was obtained from Dr. Curt Sigmund (University of Iowa, Iowa, IA) and has been described elsewhere (23).

Full-length rat Bmf cDNA was cloned from immortalized Wistar rat RPTCs (24) by conventional RT-PCR. Sense and antisense primers corresponding to nucleotides N+242 to N+265 (5′-ATG GAG CCA CCT CAG TGT GTG-3′) and N+799 to N+779 (5′-TCA CCA GGG ACC CAC CCC TTC-3′) of rat Bmf cDNA (NM_139258.1) were used in real-time PCR. Rat Bmf cDNA was subcloned into the pCMV-Myc mammalian expression vector containing the human cytomegalovirus promoter (CMV) (Clontech, Mountainview, CA), which fused an NH_2-terminal c-Myc epitope.

Generation of *db/db* transgenic mice overexpressing rat CAT. Transgenic (Tg) mice (C57Bl/6 background) overexpressing rat CAT (rCAT) in RPTCs (line #688) and homozygous *db/db* CAT-Tg mice were created in our laboratory (J.S.D.C.) and have been described previously (21,22). The *db/db* and *db/db* CAT-Tg mice were used at age 20 weeks. Non-Tg, age- and sex-matched *db/m+* littermates served as controls. The physiologic parameters of *db/m+*, *db/db*, and *db/db* CAT-Tg mice are displayed in Supplementary Table III. All animals received standard mouse chow and water ad libitum. Animal care and all procedures were approved by the CHUM animal committee.

Mouse RPT isolation and DNA microarray analysis. Animals were killed at age 20 weeks. The left and right kidneys were harvested immediately for immunohistochemistry and RPT isolation by Percoll gradient (25), respectively, as previously described (26).

Aliquots of freshly isolated mouse RPTs were immediately processed for total RNA isolation and gene chip microarray analysis. Briefly, total RNAs from three mice from each group were purified and reverse-transcribed into cDNA, which, in turn, served as the template for the generation of biotin-labeled cRNA (Enzo kit, Affymetrix, Inc., Santa Clara, CA), and then hybridized to Affymetrix Mouse Genome 430 2.0 microarray chips (Affymetrix, Inc.), according to the manufacturer's protocol. Affymetrix Mouse 430 A 2.0 chips contain ~45,000 probe sets, corresponding to more than 39,000 mouse transcripts. The data were analyzed by computer with R statistical language (version 2.51). AffylmGUI (version 1.10.5) software and the LIMMA package (version 2.10.5) of the Bioconductor Library (release 2.0) were used for data analysis (27–30). The GCRMA (Gene Chip Robust Multi-array Average) algorithm was used for background correction of the data (31), and a linear model fit was undertaken on different contrasts representing the desired group comparisons (i.e., *db/db* vs. heterozygous *db/m+* mice, *db/db* mice vs. *db/db* CAT-Tg mice). A list of normalized data (genes linked to the apoptotic pathway) from all probe sets represented on the chips was produced, and classification was performed by filtering based on $P < 0.05$. The Gene Ontology database (32) for the different probe sets served to further select genes involved in the apoptosis process with $P < 0.01$.

Real-time qPCR assays for gene expression. Total RNA was used in real-time qPCR to quantify the amount of Bmf mRNA expressed in mRPTs according to previously described methods (20). Forward (5′-CCCTTGGGGAGCAGCCCCCTG-3′) and reverse (5′-GCCGATGGAACTGGTCTGCAA-3′) primers of Bmf (NM_139258) and forward (5′-ATGCCATCCTGCGTCTGGACCTGGC-3′) and reverse (5′-AGCATTTGCGGTGCACGATGG-3′) primers of β-actin (NM_031144) were used.

Immunohistochemistry. Immunohistochemical staining for Bmf was performed by standard avidin-biotin-peroxidase complex method (ABC Staining System, Santa Cruz Biotechnology, Inc.) as previously described (20–22).

Induction of diabetes. Adult male mice (C57Bl/6 background) were rendered diabetic with STZ, as previously described (20,21). Blood glucose was monitored twice weekly; mice were killed at 4 weeks after STZ administration. Both kidneys were removed, decapsulated, and weighed together. The physiologic parameters of nondiabetic and diabetic mice are displayed in Supplementary Table IV. Left and right kidneys were processed for immunohistochemistry and RPT isolation, respectively (20–22).

Cell culture. Immortalized rat RPTCs at passages 13–18 were used in the current study using culture conditions reported previously (18,19). Briefly, the cells were synchronized for 24 h in serum-free 5 mmol/L glucose DMEM at 80–90% confluence, preincubated in 5 mmol/L glucose DMEM containing 1% depleted FBS for 30 min, and then 20 mmol/L D-mannitol (for normalization of osmolality) or 20 mmol/L D(+)-glucose were added in the absence or presence of rotenone (1×10^{-6} mol/L), DPI (5×10^{-6} mol/L), apocynin (10^{-5} mol/L), or CAT (300 units/mL). The cells were then cultured for an additional 24 h, after which they were harvested and RNA was isolated for subsequent analysis for Bmf and β-actin mRNA quantification by real-time qPCR. To analyze ROS and hydrogen peroxide (H_2O_2) generation, cells were harvested and subjected to the lucigenin assay (18,19) and H_2O_2 measurement kit (Hydrogen Peroxide Assay Kit, National Diagnostics, Atlanta, GA).

Transfections, apoptosis, and caspase-3 activity assays. The pCMV-Myc mammalian expression vector containing N-terminally Myc-tagged rat Bmf (Supplementary Fig. 1) was transiently transfected into RPTCs using Lipofectamine 2000 (InVitrogen). Cells were then incubated for 24 h in 5 mmol/L D-glucose plus 20 mmol/L D-mannitol (normal glucose) or 25 mmol/L D-glucose (HG) medium and then analyzed for apoptosis by transferase-mediated dUTP nick-end labeling (TUNEL) assay, followed by DAPI staining (TUNEL kit, Roche Diagnostics). The percentage of apoptotic RPTCs was estimated semiquantitatively. For each group, 8–9 fields (original magnification ×200) were randomly selected, and the captured TUNEL and DAPI images were overlayed using National Institutes of Health ImageJ (http://rsb.info.nih.gov/ij/) software. Cells labeled with both TUNEL and DAPI were noted as TUNEL-positive. The total number of TUNEL-positive cells was divided by the number of DAPI-stained cells and multiplied by 100 to derive the percentage of apoptotic cells per field. In some experiments, cells were harvested for caspase-3 activity assay and anti-Myc immunoblotting to confirm fusion gene expression. Caspase-3 activity was quantified fluorimetrically (20–22). Raw data were then normalized by cell lysate protein concentrations.

Coimmunoprecipitation of Myc-Bmf with Bcl-2 and Western blotting. Coimmunoprecipitation (co-IP) of Myc-Bmf with Bcl-2 was performed according to previously described methods (33).

Bmf immunostaining of kidney biopsy samples of diabetic and nondiabetic patients. Six kidney biopsy samples (paraffin sections) for immunostaining were obtained from the Department of Pathology of the CHUM. These studies were approved by the CHUM ethics committee, and all patients provided informed consent.

DNA gene chip analysis of human diabetic and nondiabetic kidneys. Human renal biopsy samples were obtained from a multicenter study, the European Renal cDNA Bank-Kröner-Fresenius-Biopsy Bank (ERCB-KFB); all patients provided informed consent according to guidelines of each respective local ethics committee. DNA gene chip analysis was performed as previously described (34–36). Twenty-five individual biopsy samples, stratified by a reference pathologist at the ERCB, were analyzed, using 18 preimplantation kidney biopsy samples from healthy living donors as control samples and 7 samples for each region of the kidney (tubules, glomeruli, etc.) from 9 DN patients with type 2 diabetes mellitus (T2DM). Samples were processed as described, and microarrays from microdissected renal compartments were hybridized to an Affy 133plus chip (34–36). Image files were processed and normalized using the ExpressionFileCreator module in GenePattern pipeline (http://genepattern.broadinstitute.org). A custom CDF (Chip Description Files) annotation file from Brainarray (http://brainarray.mbni.med.umich.edu) was used to map the probes to the respective genes based on the updated genome annotation. The normalized log-transformed data were analyzed using the significance analysis of microarray method implemented in the TM4 suite (http://www.tm4.org/mev/) to detect the differentially regulated genes between the living donors and the DN samples with a false discovery rate of <1%. The value "*q*" is a multiple testing corrected *P* value for false positives (briefly, the "*q*" value method first looks at the distribution of the *P* values, identifies at which value the *P* value becomes flattened, and then incorporates this information into the calculation of the adjusted *P* value).

Statistical analysis. Unless otherwise noted, the data are expressed as means ± SEM. Statistical analysis was performed by the *t* test provided by GraphPad Prism 5.0 software (GraphPad, San Diego, CA; http://www.graphpad.com/prism/Prism.htm). Values of $P \leq 0.05$ were considered statistically significant.

RESULTS

Microarray analysis. Normalized data of the different probe sets by setting $P < 0.05$ on the chips generated a list of 21 upregulated and 25 downregulated genes associated with apoptosis in RPTs of *db/db* mice compared with heterozygous *db/m+* or *db/db* CAT-Tg mice (Supplementary Tables I and II). Our raw and normalized data are available in the public domain Gene Expression Omnibus National Center for Biotechnology Information database (http://www.ncbi.nlm.nih.gov/geo/query/acc.cgi?acc=GSE19640).

The Gene Ontology database was used to screen for probe sets involved in apoptotic processes. Classification was further filtered by setting $P < 0.01$, compiling a list of five upregulated (Table 1) and six downregulated proapoptotic genes (Table 2) in *db/db* mice, compared with *db/m+* and *db/db* CAT-Tg mice. We chose Bmf in the current study because its expression is at least threefold

TABLE 1
Proapoptotic genes upregulated in microarray chips of *db/db* vs. *db/m+* and *db/db* vs. *db/db* CAT-Tg mice overexpressing CAT*

		db/db vs. *db/m+*		*db/db* vs. *db/db* CAT-Tg	
Probe set ID	Gene title	Fold-change	*P*	Fold-change	*P*
1450231_a_at	Baculoviral IAP repeat-containing 4	1.28	0.0039	1.29	0.0038
1454880_s_at	Bcl2-modifying factor	3.07	0.0099	3.07	0.0098
1449297_at	Caspase 12	1.82	0.0069	1.81	0.0070
1431875_a_at	E2F transcription factor 1	1.19	0.0065	1.19	0.0064
1423602_at 1445452_at	TNF receptor-associated factor 1	1.99	0.0073	1.97	0.0074

*The GO annotation package was used to select genes involved in the apoptosis process. The probe sets were selected with $P < 0.01$.

higher in RPTCs of *db/db* mice compared with *db/m+* and *db/db* CAT-Tg mice.

Validation of Bmf mRNA expression in mouse RPTs by real-time PCR. To validate the results obtained by DNA microarray, real-time qPCR was performed using primers specific for mouse Bmf mRNA. Figure 1*A* displays the results of Bmf mRNA expression in freshly isolated RPTs from *db/m+*, *db/db*, and *db/db* CAT-Tg mice. The baseline expression of Bmf mRNA in *db/db* mice was sixfold higher than in *db/m+* mice ($P < 0.005$). This increase was significantly attenuated in *db/db* CAT-Tg mice ($P < 0.05$).

Validation of Bmf expression by immunohistochemistry. We previously reported TUNEL staining on kidney sections of *db/m+*, *db/m+* CAT-Tg, *db/db*, and *db/db* CAT-Tg mice and showed that apoptotic cells were found in RPTCs of *db/db* mice but not in *db/m+*, *db/m+* CAT, and *db/db* CAT-Tgs (22). To validate whether Bmf expression was increased in RPTCs of 20-week-old T2DM *db/db* mice, immunohistochemical analysis was performed using an anti-Bmf antibody. Increased immunostaining for Bmf was observed in the RPTCs of diabetic *db/db* mice (Fig. 1*B*, *b*) compared with the RPTCs of nondiabetic *db/m*$^+$ control mice (Fig. 1*B*, *a*). CAT overexpression effectively attenuated Bmf expression, as observed in RPTs of *db/db* CAT-Tg mice (Fig. 1*B*, *c*). No immunostaining was observed with nonimmune control serum in *db/db* mice (Fig. 1*B*, *d*). Quantification of Bmf immunostaining confirmed enhanced Bmf expression in RPTCs of *db/db* mice (Fig. 1*C*). Similarly, kidneys from adult mice with STZ-induced diabetes also exhibited enhanced Bmf immunostaining in RPTCs (Fig. 2*A*, *b* and *B*) compared with nondiabetic littermates (Fig. 2*A*, *a* and *B*). Treatment of diabetic mice with insulin reduced Bmf expression to control levels (Fig. 2*A*, *c* and *B*). No immunostaining was observed in sections treated with nonimmune control serum (Fig. 2*A*, *d*). These results were further validated by performing real-time qPCR for Bmf using RNA isolated from RPTCs of STZ-induced diabetic mice. Figure 2*C* shows a significant increase ($P < 0.05$) in Bmf mRNA expression levels in STZ-induced diabetic mice compared with control and insulin-treated STZ-injected mice.

HG induces ROS generation and Bmf mRNA expression in RPTCs in vitro. Immortalized rat RPTCs were cultured in normal glucose or HG medium with or without rotenone, CAT, DPI, or apocynin. Cells were then harvested to assess ROS generation with the lucigenin assay, and RNA was isolated for real-time qPCR analysis. RPTCs cultured in HG produced significantly higher amounts of ROS than RPTCs cultured in normal glucose (Fig. 3*A*), and these increases could be markedly attenuated or inhibited by rotenone, CAT, DPI, or apocynin. Furthermore, RPTCs cultured in HG medium exhibited fourfold higher Bmf mRNA expression than RPTCs cultured in normal glucose medium ($P \leq 0.01$; Fig. 3*B*). The HG-stimulated increases in Bmf mRNA expression were inhibited by rotenone, CAT, DPI, and apocynin.

TGF-β1 upregulates Bmf mRNA expression in rat RPTCs. To investigate the mechanism(s) of HG-stimulation of Bmf expression, RPTCs were cultured with active human TGF-β1 in normal glucose medium. TGF-β1 increased Bmf mRNA expression in a concentration-dependent manner (Fig. 3*C*). Conversely, knockdown of TGF-β1 with siRNA attenuated HG-stimulation of Bmf mRNA expression in RPTCs (Fig. 3*D*).

Cloning and amino acid sequence of rat Bmf. We cloned Bmf cDNA from rat RPTCs (Wistar strain) by conventional RT-PCR. Rat and mouse Bmf consists of 185 amino acids and is 98.9% homologous. Rat Bmf cDNA was then subcloned into the pCMV-Myc mammalian expression vector, which fused an NH_2-terminal c-Myc epitope tag (Supplementary Fig. 1*A* and *B*).

Bmf overexpression leads to activation of caspase-3 and RPTC apoptosis. To study the role of Bmf in apoptosis, rat RPTCs were transiently transfected with NH_2-terminally Myc-tagged Bmf or an empty vector, and

TABLE 2
Proapoptotic genes downreguated in microarray chips of *db/db* vs. *db/m+* and *db/db* vs. *db/db* CAT-Tg mice overexpressing CAT*

		db/db vs. *db/m+*		*db/db* vs. *db/db* CAT-Tg	
Probe set ID	Gene title	Fold-change	*P*	Fold-change	*P*
1417962_s_at	Growth hormone receptor	−2.92	0.0031	−3.44	0.0024
1419592_at	Unc-5 homolog C (C. elegans)	−1.53	0.0058	−1.39	0.0090
1435369_at	U box domain-containing 5	−2.10	0.0012	−1.84	0.0016
1451845_a_at	Peptidyl-tRNA hydrolase 2	−1.88	0.0018	−1.32	0.0087
1452172_at	FAST kinase domains 2	−2.10	0.0013	−1.60	0.0027
1460671_at	Glutathione peroxidase 1	−1.41	0.0091	−1.51	0.0063

*The GO annotation package was used to select genes involved in the apoptosis process. The probe sets were selected with $P < 0.01$.

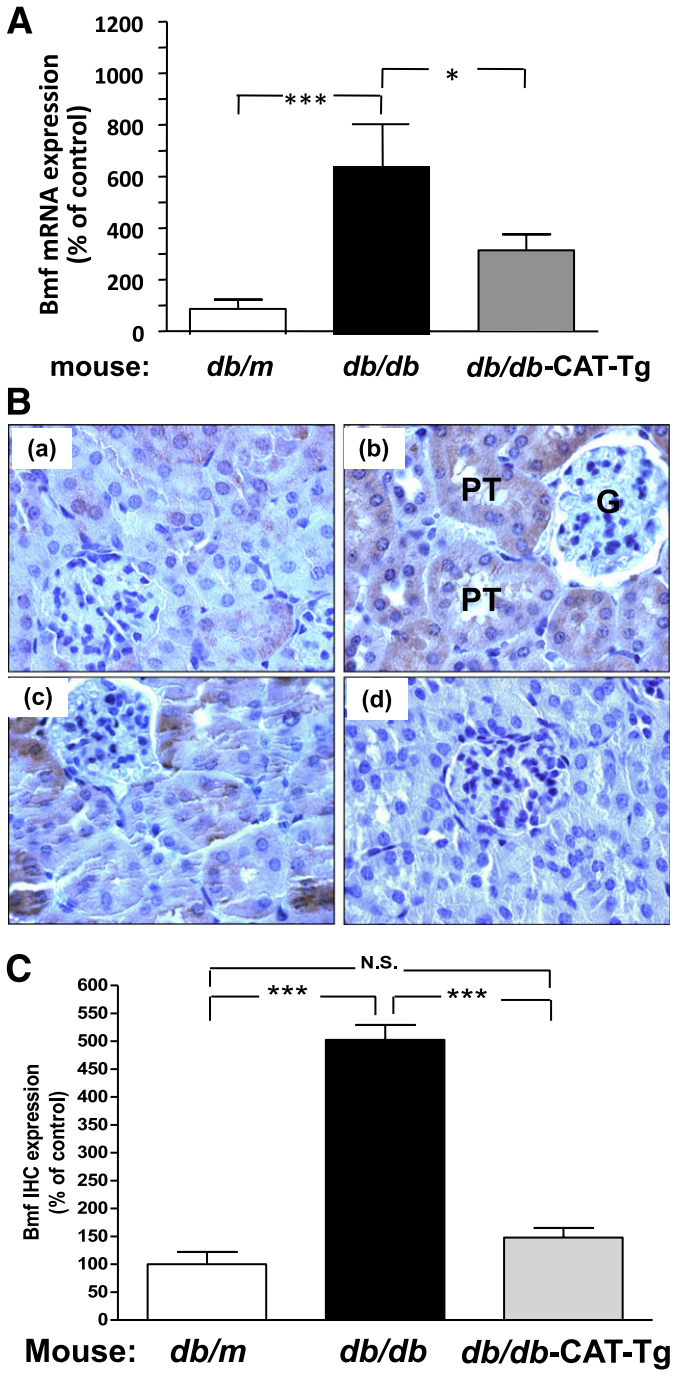

FIG. 1. Bmf expression is elevated in RPTs of *db/db* diabetic mice. *A*: Real-time qPCR for Bmf mRNA levels in freshly isolated RPTs from *db/m*, *db/db*, and *db/db* CAT-Tg mice. Values were corrected to β-actin. *B*: Bmf immunohistochemical (IHC) staining in kidney sections (original magnification ×600) from (*a*) *db/m*$^{+}$, (*b*) *db/db*, and (*c*) *db/db* CAT-Tg mice; (*d*) presents a nonimmune rabbit serum control. G, Glomerulus. *C*: Quantification of Bmf IHC staining. Values are the mean ± SEM, n = 5–7 for each group. *$P < 0.05$; ***$P < 0.005$. N.S., not significant. (A high-quality color representation of this figure is available in the online issue.)

caspase-3 activity was determined in cell lysates. Expression of the fusion protein was confirmed by RT-PCR (Fig. 4*A*) and anti-Myc immunoblotting (Fig. 4*B*). Caspase-3 activity was significantly increased in lysates from cells transiently transfected with the Bmf fusion protein compared with lysates from cells transiently transfected with empty vector ($P < 0.005$). Caspase-3 activity was further augmented

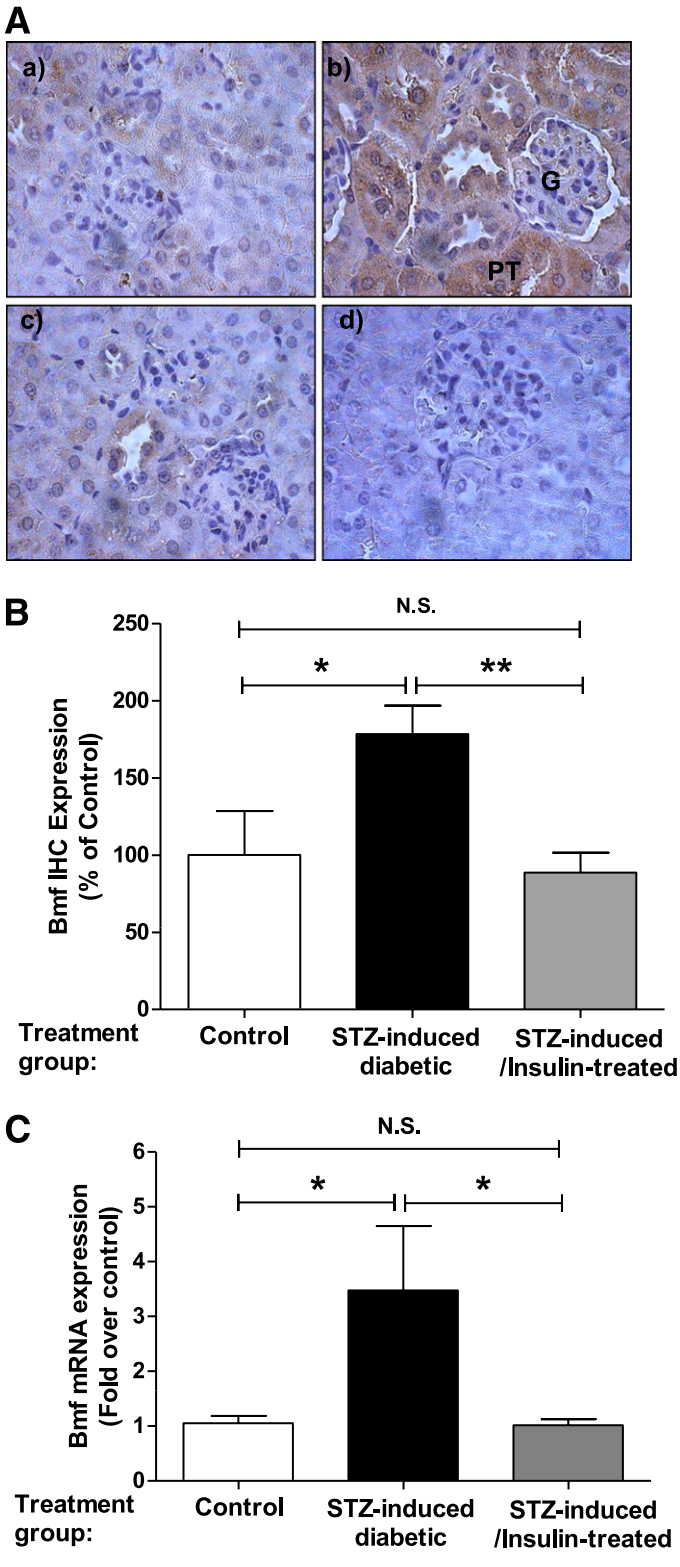

FIG. 2. Bmf expression is upregulated in RPTs from STZ-induced diabetic mouse kidneys. *A*: Bmf immunohistochemical (IHC) staining in kidney sections (original magnification ×600) from nondiabetic control (*a*), STZ-induced diabetic (*b*), and insulin-treated STZ-injected mice (*c*); nonimmune rabbit serum control is also presented (*d*). *B*: Quantification of Bmf-IHC. Values are the mean ± SEM, n = 4–12. *C*: Real-time qPCR for Bmf mRNA levels in freshly isolated RPTs from control and STZ-induced diabetic and insulin-treated STZ-injected mice. Values were corrected to β-actin. *$P < 0.05$; **$P < 0.01$. N.S., not significant. (A high-quality color representation of this figure is available in the online issue.)

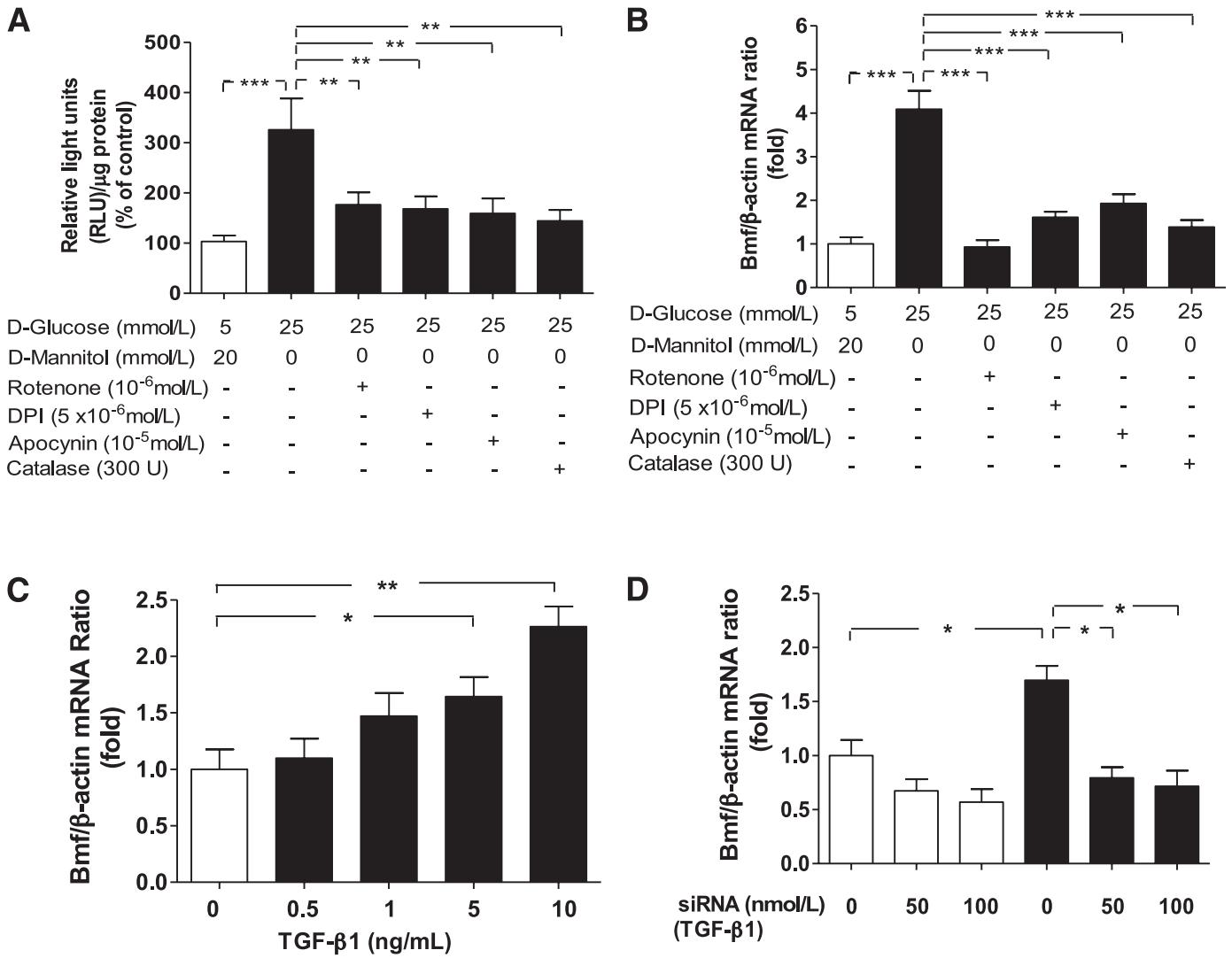

FIG. 3. HG stimulates ROS generation and Bmf mRNA expression in rat RPTCs in vitro. *A*: ROS generation of RPTCs cultured in normal glucose (5 mmol/L D-glucose plus 20 mmol/L D-mannitol) and HG (25 mmol/L D-glucose) media with various inhibitors, as indicated. Values are corrected to lysate protein levels. *B*: Real-time qPCR for Bmf mRNA levels in RPTCs in vitro after treatment with normal glucose or HG and various inhibitors, as indicated. *C*: Real-time qPCR for Bmf mRNA levels in RPTCs in response to active human TGF-β1. *D*: Real-time qPCR for Bmf mRNA levels in RPTCs in vitro after transfection with siRNA of TGF-β1 or scrambled siRNA in normal glucose (□) and HG (■) media. Values are corrected to β-actin levels. *$P < 0.05$; **$P < 0.01$; ***$P < 0.005$; N.S., not significant.

when RPTCs were cultured in HG medium ($P < 0.005$; Fig. 4*C*). Knockdown of Bmf with siRNA reduced HG-induced apotposis (TUNEL assay) in RPTCs compared with scrambled siRNA (Fig. 4*D*).

RPTCs transiently transfected with NH_2-terminally Myc-tagged Bmf exhibited fourfold increase in TUNEL-positive cells compared with empty vector-transfected cells ($P < 0.005$; Fig. 5*A*, and *B*). Parallel assays with lysates from transfected cells confirmed the expression of Myc-tagged Bmf (Fig. 5*C*).

Bmf interacts with Bcl-2 in rat IRPTCs. To investigate Bmf interaction with Bcl-2, coimmunoprecipitation experiments of Myc-Bmf with Bcl-2 were performed. Significant increases in coimmunoprecipitated Bcl-2 (Fig. 5*D*, *a*) but not Myc-Bmf (Fig. 5*D*, *b*) were observed in rat IRPTCs overexpressing Myc-Bmf cultured in HG medium.

Bmf expression in diabetic human kidneys. The clinical characteristics of the patients are shown in Supplementary Table VI. All had kidney cancer, which was the reason for the nephrectomies; some had T2DM, but others did not. Immunohistochemistry revealed Bmf expression in the renal distal tubules but not in the renal proximal tubules (RPTs) of the normal portions of human nephrectomy specimens from nondiabetic patients with kidney cancer (Fig. 6*A*, *a–c*). However, increased immunostaining for Bmf was observed in RPTs of the normal portions of nephrectomy specimens from patients with kidney cancer who also had diabetes (Fig. 6*A*, *d–f*). Interestingly, double immunostaining revealed frequent colocalization of Bmf overexpression in TUNEL-positive apoptotic RPTCs in diabetic kidney but not in nondiabetic kidney (Fig. 6*B*).

DNA gene chip microarray analysis (Affymetrix Gene Chip HGU 133plus 2 chip) of microdissected nephrons from seven patients with T2DM revealed modestly but significantly enhanced Bmf expression in glomeruli (1.48-fold increase) and tubulointerstitium (1.39-fold increase) compared with 18 control biopsy specimens from kidneys from living donors taken at the time of transplant ($q < 0.01$, where q value is a multiple-testing corrected

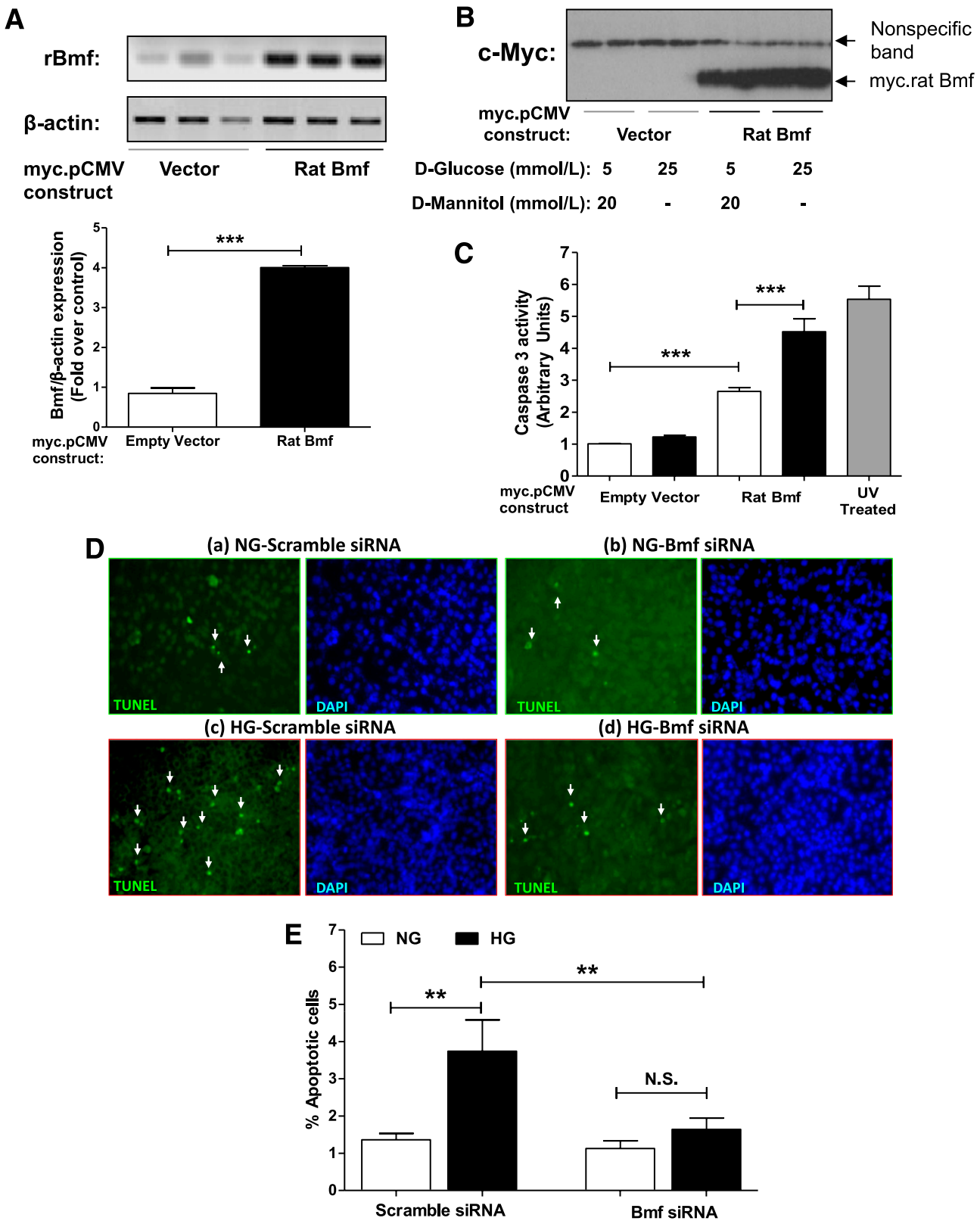

FIG. 4. Overexpression of rat Bmf induces caspase-3 activity in rat RPTCs in vitro. ***A***: RPTCs were transiently transfected by lipofectamine 2000 with the empty vector, pCMV-Myc or plasmid containing NH_2-terminally tagged rat Bmf cDNA (pCMV-Myc rat Bmf). Expression of the Myc-rat Bmf mRNA was confirmed by conventional RT-PCR and quantified by densitometry. ***B***: Anti-Myc immunoblotting was also performed. The nonspecific band serves as loading control. ***C***: Caspase 3 activity in RPTCs transfected with empty vector (pCMV-Myc) or pCMV-Myc rat Bmf in normal glucose (□) and HG (■) media. Values are corrected to lysate protein levels. Values are the mean ± SEM, n = 4–8. ***P < 0.005. UV, ultraviolet. ***D***: TUNEL images (***a–d***) and quantification of apoptotic cells (***E***) in vitro. After transfection with scrambled siRNA (***a*** and ***c***) or Bmf siRNA (***b*** and ***d***) in RPTCs cultured in normal glucose (NG, ***a*** and ***b***) or HG (***c*** and ***d***) medium, cells were fixed and subjected to TUNEL (green) and DAPI (blue) staining (original magnification ×200). White arrows indicate TUNEL-positive cells; (***e***) quantification of TUNEL-positive cells (n = 3 experiments). **P < 0.01; N.S., not significant. (A high-quality color representation of this figure is available in the online issue.)

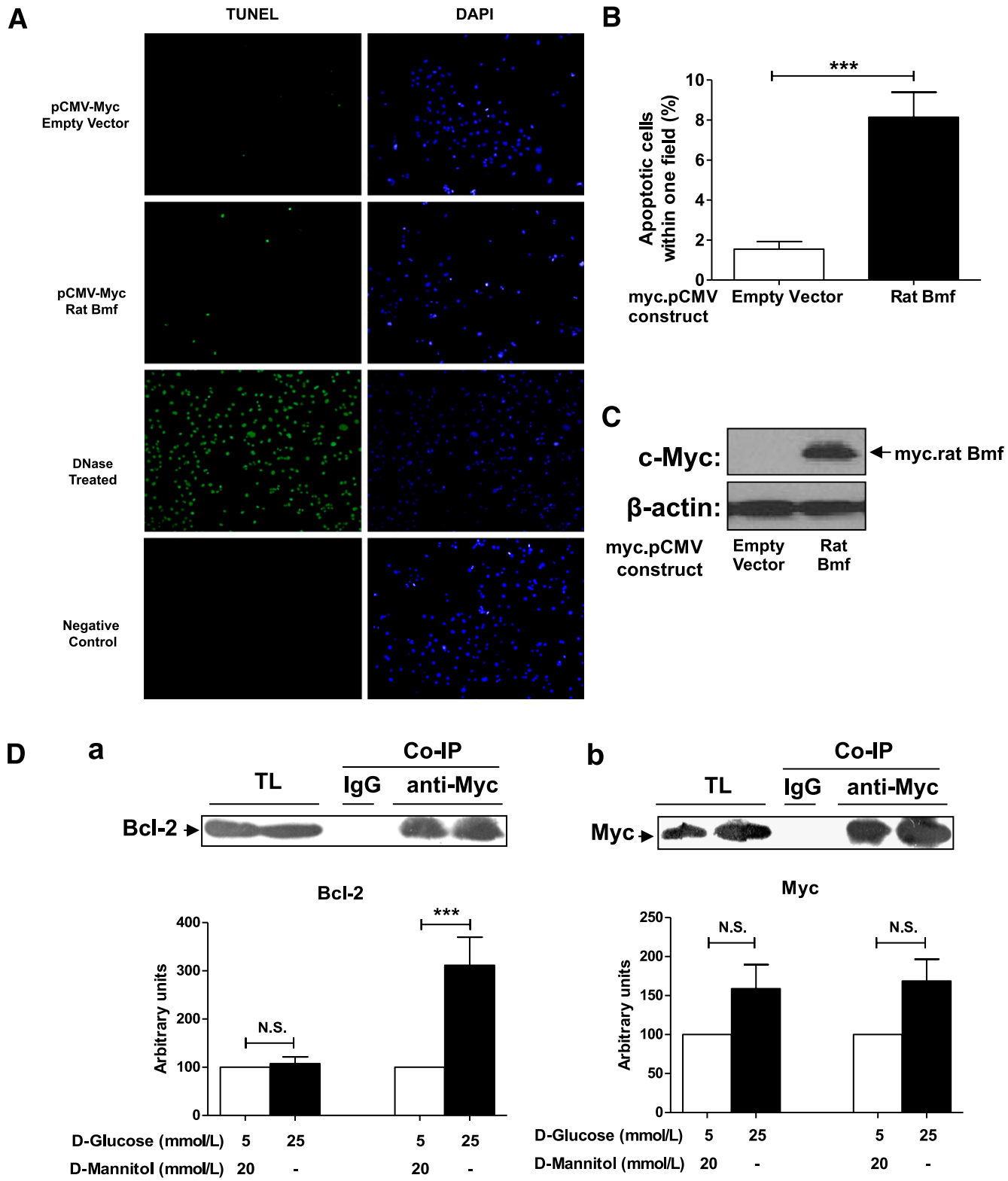

FIG. 5. Overexpression of rat Bmf increases TUNEL-positive cells and coimmunoprecipitates (Co-IP) with Bcl-2 in rat RPTCs in vitro. *A*: RPTCs were transiently transfected with the empty vector, pCMV-Myc, or pCMV-Myc rat Bmf. Cells were incubated for 24 h in 25 mmol/L D-glucose, then fixed and subjected to TUNEL and DAPI staining. TUNEL (green) and DAPI (blue) staining (original magnification ×200) are shown for RPTCs transfected with empty vector and pCMV-Myc rat Bmf. DNase-treated cells serve as TUNEL-positive controls. Cells left untreated with terminal transferase serve as a TUNEL-negative control. *B*: Quantification of TUNEL-positive cells per field is shown. Values are presented as percentages of TUNEL-positive cells/total cells per field ± SEM (n = 8 or 9). ***P < 0.005. *C*: Expression of the Myc-rat Bmf fusion protein was confirmed by anti-Myc immunoblotting, with β-actin as the loading control. *D*: Interaction of Myc-Bmf with Bcl-2 in rat RPTCs: (*a*) Immunoblotting for Bcl-2 in cytosolic fractions of rat RPTCs before (total lysate, TL) and after Co-IP with anti-Myc; (*b*) immunoblotting for Myc in cytosolic fractions of rat RPTCs on the same membrane after immunobotting for anti-Bcl-2 in panel *a*. The relative density of Bcl-2 or Myc in RPTCs cultured normal glucose (5 mmol/L D-glucose plus 20 mmol/L D-mannitol DMEM) was expressed as controls (100 arbitrary units). Rabbit purified IgG (3 μg) was used as the control for Co-IP experiments. Values are the mean ± SEM for 4 independent experiments. ***P < 0.005; N.S., not significant. □, normal glucose; ■, high glucose medium. (A high-quality digital representation of this figure is available in the online issue.)

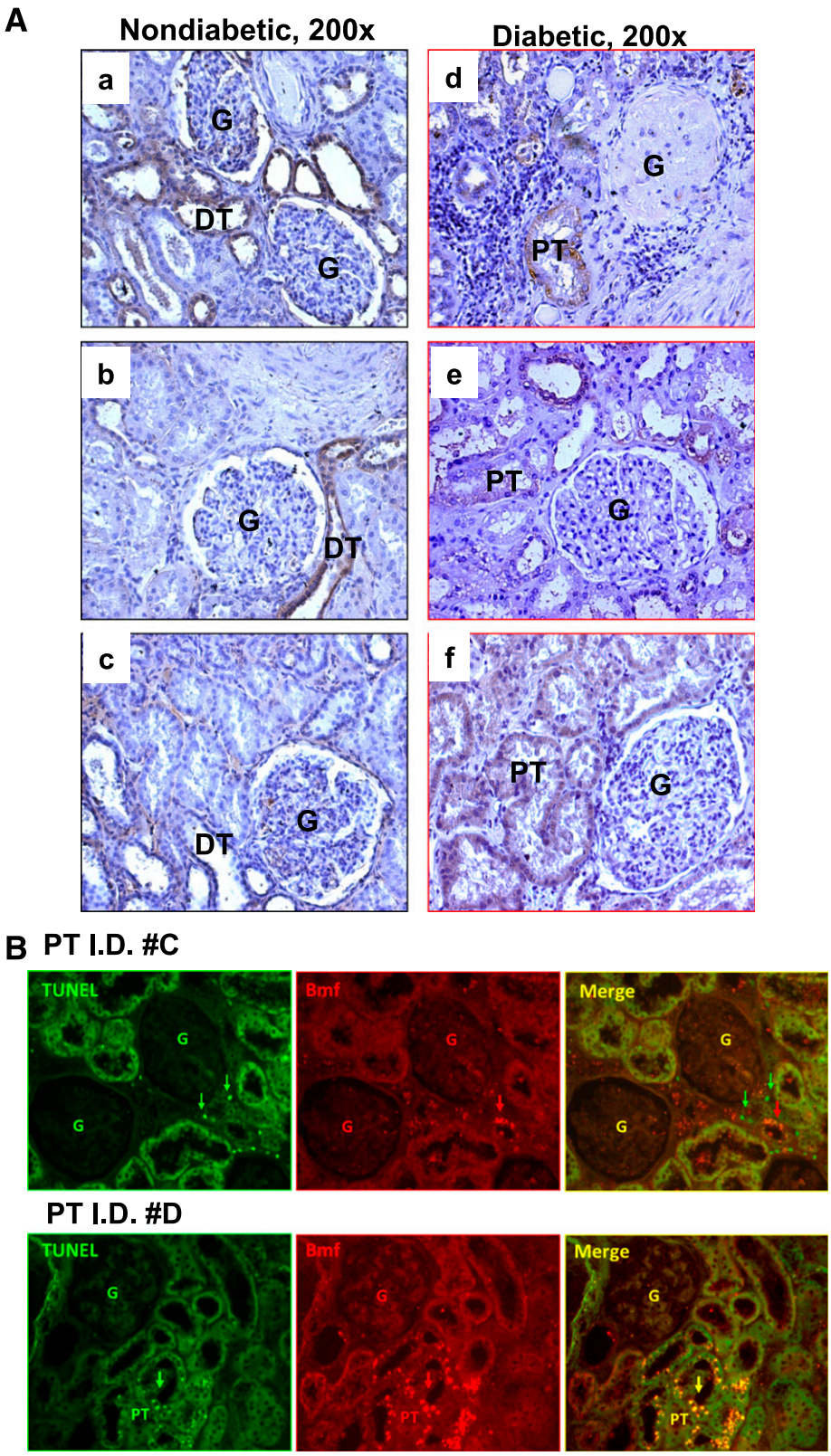

FIG. 6. Enhanced Bmf expression in RPTs from human kidneys from patients with diabetes. *A*: Bmf immunohistochemical staining in human kidney sections (original magnification ×200) from three nondiabetic cancer patients (*a*, patient with papillary variant carcinoma; *b*, patient with clear cell carcinoma; and *c*, patient with thyroid-like renal carcinoma) and three diabetic cancer patients (*d*, patient with papillary variant carcinoma and evidence of DN [nodular with tubular atrophy and interstitial fibrosis]; *e*, patient with clear cell carcinoma and no evidence of DN; and *f*, patient with clear cell carcinoma and nephroangiosclerosis with evidence of DN [secondary focal glomerulosclerosis, tubular atrophy, and interstitial fibrosis]). DT, distal tubule; G, glomerulus. *B*: Colocalization of Bmf expression and TUNEL-positive cells in human kidneys. Nondiabetic human kidney (patient I.D. #C,) and diabetic human kidney with DN (patient I.D. #D) were sectioned, subjected to TUNEL assay to visualize apoptotic cells (green), and then incubated with anti-Bmf antibody, followed by anti-goat AlexaFluor 594 to demonstrate Bmf expression (red). Cells staining positively for TUNEL and Bmf appear yellow (merged image). Original magnification ×200. Arrows indicate cells that stained positively for TUNEL and Bmf. G, glomerulus; DT, distal tubule. (A high-quality color representation of this figure is available in the online issue.)

P value). Supplementary Table VII summarizes the clinical characteristics of the patients in the gene microarray analysis.

DISCUSSION

The current study documents enhanced Bmf expression in RPTCs of *db*/*db* mice, STZ-induced diabetic mice, and kidneys from patients with T2DM and shows that Bmf overexpression enhances RPTC apoptosis, indicating a potential role for Bmf in mediating tubular atrophy in the diabetic kidney.

To identify the proapoptotic genes regulated by ROS in *db*/*db* mice RPTCs, we used gene chip microarrays as an initial screen (37). A combination of high *P* values, fold changes, and Gene Ontology annotation (32) allowed us to obtain an overview of the genetic regulation of RPTC apoptosis occurring in murine models of T2DM.

We identified Bmf as one of five putative proapoptotic genes that were differentially upregulated ($P < 0.01$ and >1.5-fold increase) in RPTs of *db*/*db* mice compared with *db*/*m*+ and *db*/*db* CAT-Tg mice. The upregulation of Bmf mRNA and protein expression in RPTCs of *db*/*db* mice was confirmed by real-time qPCR and immunostaining.

To confirm enhanced Bmf expression, we used another model of diabetes, STZ-induced diabetes in mice (20). Our results document significant upregulation of Bmf expression in RPTCs of STZ-induced diabetes and its reversal by insulin.

There is evidence that HG induces apoptosis in RPTCs via ROS generation (20,38). Our present data show that HG also stimulates Bmf mRNA expression, which can be inhibited by rotenone, CAT, DPI, and apocynin. Cellular H_2O_2 and mitochondrial ROS levels were also significantly higher in RPTCs incubated in HG medium than in RPTCs cultured in normal glucose and were normalized in the presence of CAT (Supplementary Fig 2*a* and *b*). These observations indicate that ROS derived from mitochondrial oxidative metabolism may mediate, at least in part, HG-induced Bmf expression, which in turn would promote RPTC apoptosis.

To provide evidence that Bmf can directly induce RPTC apoptosis, we overexpressed Bmf in rat RPTCs. Transient transfection of RPTCs with rat Bmf cDNA resulted in activation of caspase-3 parallel with increases in the number of apoptotic cells, similar to that observed in transfected fibroblasts and cancer cells (39). We were unable to detect increases in endogenous rat Bmf expression in RPTCs by immunoblotting or immunofluorescence (data not shown) using the same anti-Bmf antibodies used for immunohistochemistry. Of note, Schmelzle et al. (40) also observed that commercially available anti-Bmf antibodies do not work in immunoblotting versus immunohistochemistry of Bmf.

The precise mechanism(s) by which HG evokes Bmf expression in RPTC apoptosis remains unclear. Our present data show that TGF-β1 stimulates Bmf mRNA expression and that knockdown of TGF-β1 with siRNA attenuates Bmf mRNA expression in RPTCs in HG. These observations are consistent with findings of Ramjaun et al. (41) showing that TGF-β1 stimulates *Bmf* gene expression. ROS could induce phosphorylation of Bmf via c-Jun NH_2-terminal kinase (42) or other signaling pathways. Phosphorylated Bmf would then translocate from the cytoskeleton to bind antiapoptotic proteins (i.e., Bcl-2 and Bcl-xL), which are located on the mitochondria, to interfere with Bcl-2/Bcl-xL mitochondrial gatekeeping and thus allow enhanced Bax binding to the mitochondrion. This would result in the collapse of the mitochondrial transmembrane potential and thus activation of the intrinsic pathway of apoptosis. Our findings that Myc-Bmf coimmunoprecipitates Bcl-2 in rat RPTCs lend further support to this notion.

We searched the publicly accessible National Center for Biotechnology Information data bank (http://www.ncbi.nlm.nih.gov/geo/query/acc.cgi?acc=GSE1009) for microarray studies performed on biopsy specimens from patients with DN (Supplementary Table V) to confirm our findings in *db*/*db* mice. Bmf was not detectable, however, in human kidneys from patients with diabetes when the first generation of chips (Affymetrix Human Genome U95 Version 2 Array) was used because a Bmf probeset was not present in these chips. Bmf expression was upregulated, however, in kidney allografts from living donors compared with at implantation before revascularization (0 months) using the Affymetrix Human Genome U133 Plus 2.0 Array (Affy 133plus chip), which contains the Bmf probeset. These findings indicate that Bmf expression may be upregulated in human kidneys under pathologic conditions, including DN.

Indeed, this possibility is supported by our immunohistochemistry studies that show increased Bmf expression in RPTs taken from nonmalignant portions of kidneys removed removed from diabetic patients due to kidney cancer compared with those taken from nondiabetic patients with kidney cancer. Interestingly, RPTCs overexpressing Bmf frequently stained positive for TUNEL in diabetic human kidney. Furthermore, the Affy 133plus chip assay revealed significantly upregulated Bmf expression ($q < 0.01$, where *q* value is a multiple testing corrected *P* value) in microdissected glomeruli (1.48-fold increase) and tubulointerstitium (1.39-fold increase) from patients with T2DM compared with nondiabetic patients (kidney donors). The 1.39-fold versus 3-fold increases in Bmf expression in human diabetic tubulointerstitium and *db*/*db* mice RPTs, respectively, are difficult to reconcile. It is possible that Bmf mRNA expression in human tubulointestitium might have been underestimated because of the use of a mixture of tubules and interstitium versus the >90% purity of our *db*/*db* mouse RPT fraction. Additional qPCR studies are needed to compare Bmf expression in human RPTs with or without T2DM.

Our results may have clinical implications for patients with T2DM. Because tubular apoptosis is one of the characteristic morphologic changes in human diabetic kidneys (15–17) and tubular atrophy appears to be a better indicator of disease progression than glomerular pathology (2–4), we suggest that RPTC apoptosis may be an initial mechanism for tubular atrophy in T2DM. Our present data point toward Bmf as one of the mediators of this process. However, whether enhanced Bmf expression directly or indirectly induces RPTC apoptosis in human T2DM remains to be investigated.

In summary, the current study suggests an important role for Bmf in mediating RPTC apoptosis in the diabetic mouse kidney in vivo, and, likely, in diabetic human kidneys. Our observations raise the possibility that selective targeting of this proapoptotic protein may provide a novel approach in preventing or reversing the pathologic manifestations of DN, particularly tubular atrophy.

ACKNOWLEDGMENTS

This work was supported, in part, by grants from the Canadian Institutes of Health Research (MOP 84363 and MOP 106688) to J.S.D.C., the Kidney Foundation of Canada

(KFOC80015) to J.S.D.C., and the National Institutes of Health (HL-48455) to J.R.I. M.K. and V.N. were supported by P30 DK081943-01 (Applied System Biology Core, O'Brien Renal Center, University of Michigan), and C.D.C. was supported by the Else Kröner-Fresenius Foundation.

No potential conflicts of interest relevant to this article were reported.

G.J.L. and N.G. researched data, contributed to discussion, and wrote the manuscript. H.M., C.-S.L., S.-J.W., J.-X.Z., M.-L.B., I.C., J.F.-M., J.-B.L., V.N., and C.D.C. researched data. J.E., M.K., and S.-L.Z. researched data and contributed to discussion. J.G.F. and J.R.I. contributed to discussion and reviewed and edited manuscript. J.S.D.C. contributed to discussion and wrote, reviewed, and edited the manuscript.

The authors thank all participating centers of the European Renal cDNA Bank-Kroener-Fresenius biopsy bank (ERCB-KFB) and their patients for their cooperation. Active members at the time of the study: Clemens David Cohen, Holger Schmid, Michael Fischereder, Lutz Weber, Matthias Kretzler, Detlef Schlöndorff, Munich/Zurich/Ann Arbor/New York; Jean Daniel Sraer, Pierre Ronco, Paris; Maria Pia Rastaldi, Giuseppe D'Amico, Milano; Peter Doran, Hugh Brady, Dublin; Detlev Mönks, Christoph Wanner, Würzburg; Andy Rees, Aberdeen; Frank Strutz, Gerhard Anton Müller, Göttingen; Peter Mertens, Jürgen Floege, Aachen; Norbert Braun, Teut Risler, Tübingen; Loreto Gesualdo, Francesco Paolo Schena, Bari; Jens Gerth, Gunter Wolf, Jena; Rainer Oberbauer, Dontscho Kerjaschki, Vienna; Bernhard Banas, Bernhard Krämer, Regensburg; Moin Saleem, Bristol; Rudolf Wüthrich, Zurich; Walter Samtleben, Munich; Harm Peters, Hans-Hellmut Neumayer, Berlin; Mohamed Daha, Leiden; Katrin Ivens, Bernd Grabensee, Düsseldorf; Francisco Mampaso (deceased), Madrid; Jun Oh, Franz Schaefer, Martin Zeier, Hermann-Joseph Gröne, Heidelberg; Peter Gross, Dresden; Giancarlo Tonolo; Sassari; Vladimir Tesar, Prague; Harald Rupprecht, Bayreuth; and Hans-Peter Marti, Bern.

Parts of this study were presented as a free communication at the Annual Meeting of the American Society of Nephrology, Philadelphia, PA, 4–9 November 2008.

REFERENCES

1. Nangaku M. Mechanisms of tubulointerstitial injury in the kidney: final common pathways to end-stage renal failure. Intern Med 2004;43:9–17
2. Gilbert RE, Cooper ME. The tubulointerstitium in progressive diabetic kidney disease: more than an aftermath of glomerular injury? Kidney Int 1999;56:1627–1637
3. Marcussen N. Tubulointerstitial damage leads to atubular glomeruli: significance and possible role in progression. Nephrol Dial Transplant 2000;15 (Suppl. 6):74–75
4. Drummond K, Mauer M; International Diabetic Nephropathy Study Group. The early natural history of nephropathy in type 1 diabetes: II. Early renal structural changes in type 1 diabetes. Diabetes 2002;51: 1580–1587
5. Beyenbach KW. Kidneys sans glomeruli. Am J Physiol Renal Physiol 2004; 286:F811–F827
6. Najafian B, Kim Y, Crosson JT, Mauer M. Atubular glomeruli and glomerulotubular junction abnormalities in diabetic nephropathy. J Am Soc Nephrol 2003;14:908–917
7. Najafian B, Crosson JT, Kim Y, Mauer M. Glomerulotubular junction abnormalities are associated with proteinuria in type 1 diabetes. J Am Soc Nephrol 2006;17(Suppl. 2):S53–S60
8. Han HJ, Lee YJ, Park SH, Lee JH, Taub M. High glucose-induced oxidative stress inhibits Na+/glucose cotransporter activity in renal proximal tubule cells. Am J Physiol Renal Physiol 2005;288:F988–F996
9. Thevenod F. Nephrotoxicity and the proximal tubule. Insights from cadmium. Nephron Physiol 2003;93:p87–p93
10. Rogers LK, Bates CM, Welty SE, Smith CV. Diquat induces renal proximal tubule injury in glutathione reductase-deficient mice. Toxicol Appl Pharmacol 2006;217:289–298
11. de Haan JB, Stefanovic N, Nikolic-Paterson D, et al. Kidney expression of glutathione peroxidase-1 is not protective against streptozotocin-induced diabetic nephropathy. Am J Physiol Renal Physiol 2005;289: F544–F551
12. Zhang Y, Wada J, Hashimoto I, et al. Therapeutic approach for diabetic nephropathy using gene delivery of translocase of inner mitochondrial membrane 44 by reducing mitochondrial superoxide production. J Am Soc Nephrol 2006;17:1090–1101
13. Kumar D, Zimpelmann J, Robertson S, Burns KD. Tubular and interstitial cell apoptosis in the streptozotocin-diabetic rat kidney. Nephron Exp Nephrol 2004;96:e77–e88
14. Kelly DJ, Stein-Oakley A, Zhang Y, et al. Fas-induced apoptosis is a feature of progressive diabetic nephropathy in transgenic (mRen-2)27 rats: attenuation with renin-angiotensin blockade. Nephrology (Carlton) 2004; 9:7–13
15. Susztak K, Ciccone E, McCue P, Sharma K, Böttinger EP. Multiple metabolic hits converge on CD36 as novel mediator of tubular epithelial apoptosis in diabetic nephropathy. PLoS Med 2005;2:e45
16. Kumar D, Robertson S, Burns KD. Evidence of apoptosis in human diabetic kidney. Mol Cell Biochem 2004;259:67–70
17. Verzola D, Gandolfo MT, Ferrario F, et al. Apoptosis in the kidneys of patients with type II diabetic nephropathy. Kidney Int 2007;72:1262–1272
18. Hsieh TJ, Zhang SL, Filep JG, Tang SS, Ingelfinger JR, Chan JSD. High glucose stimulates angiotensinogen gene expression via reactive oxygen species generation in rat kidney proximal tubular cells. Endocrinology 2002;143:2975–2985
19. Hsieh TJ, Fustier P, Zhang S-L, et al. High glucose stimulates angiotensinogen gene expression and cell hypertrophy via activation of the hexosamine biosynthesis pathway in rat kidney proximal tubular cells. Endocrinology 2003;144:4338–4349
20. Liu F, Brezniceanu M-L, Wei C-C, et al. Overexpression of angiotensinogen increases tubular apoptosis in diabetes. J Am Soc Nephrol 2008; 19:269–280
21. Brezniceanu ML, Liu F, Wei C-C, et al. Catalase overexpression attenuates angiotensinogen expression and apoptosis in diabetic mice. Kidney Int 2007;71:912–923
22. Brezniceanu M-L, Liu F, Wei CC, et al. Attenuation of interstitial fibrosis and tubular apoptosis in db/db transgenic mice overexpressing catalase in renal proximal tubular cells. Diabetes 2008;57:1–9
23. Ding Y, Davisson RL, Hardy DO, et al. The kidney androgen-regulated protein promoter confers renal proximal tubule cell-specific and highly androgen-responsive expression on the human angiotensinogen gene in transgenic mice. J Biol Chem 1997;272:28142–28148
24. Ingelfinger JR, Jung F, Diamant D, et al. Rat proximal tubule cell line transformed with origin-defective SV40 DNA: autocrine ANG II feedback. Am J Physiol 1999;276:F218–F227
25. Vinay P, Gougoux A, Lemieux G. Isolation of a pure suspension of rat proximal tubules. Am J Physiol 1981;241:F403–F411
26. Brezniceanu ML, Wei C-C, Zhang S-L, et al. Transforming growth factor-beta 1 stimulates angiotensinogen gene expression in kidney proximal tubular cells. Kidney Int 2006;69:1977–1985
27. Smyth GK. Linear models and empirical bayes methods for assessing differential expression in microarray experiments. Stat Appl Genet Mol Biol 2004;3:Article3
28. Smyth GK, Michaud J, Scott HS. Use of within-array replicate spots for assessing differential expression in microarray experiments. Bioinformatics 2005;21:2067–2075
29. Wettenhall JM, Simpson KM, Satterley K, Smyth GK. affylmGUI: a graphical user interface for linear modeling of single channel microarray data. Bioinformatics 2006;22:897–899
30. Gentleman RC, Carey VJ, Bates DM, et al. Bioconductor: open software development for computational biology and bioinformatics. Genome Biol 2004;5:R80.1–R80.16
31. Wu Z, Irizarry R, Gentleman R, Martinez-Murillo F, Spencer F. A model-based background adjustment for oligonucleotide expression arrays. J Am Stat Assoc 2004;99:909–917
32. Ashburner M, Ball CA, Blake JA, et al.; The Gene Ontology Consortium. Gene ontology: tool for the unification of biology. Nat Genet 2000;25:25–29
33. Liu F, Wei CC, Wu SJ, et al. Apocynin attenuates tubular apoptosis and tubulointerstitial fibrosis in transgenic mice independent of hypertension. Kidney Int 2009;75:156–166
34. Cohen CD, Frach K, Schlöndorff D, Kretzler M. Quantitative gene expression analysis in renal biopsies: a novel protocol for a high-throughput multicenter application. Kidney Int 2002;61:133–140

35. Lindenmeyer MT, Kretzler M, Boucherot A, et al. Interstitial vascular rarefaction and reduced VEGF-A expression in human diabetic nephropathy. J Am Soc Nephrol 2007;18:1765–1776
36. Schmid H, Boucherot A, Yasuda Y, et al.; European Renal cDNA Bank (ERCB) Consortium. Modular activation of nuclear factor-kappaB transcriptional programs in human diabetic nephropathy. Diabetes 2006; 55:2993–3003
37. Susztak K, Böttinger EP. Diabetic nephropathy: a frontier for personalized medicine. J Am Soc Nephrol 2006;17:361–367
38. Allen DA, Harwood S, Varagunam M, Raftery MJ, Yaqoob MM. High glucose-induced oxidative stress causes apoptosis in proximal tubular epithelial cells and is mediated by multiple caspases. FASEB J 2003;17: 908–910
39. Morales AA, Olsson A, Celsing F, Osterborg A, Jondal M, Osorio LM. Expression and transcriptional regulation of functionally distinct Bmf isoforms in B-chronic lymphocytic leukemia cells. Leukemia 2004;18:41–47
40. Schmelzle T, Mailleux AA, Overholtzer M, et al. Functional role and oncogene-regulated expression of the BH3-only factor Bmf in mammary epithelial anoikis and morphogenesis. Proc Natl Acad Sci USA 2007;104: 3787–3792
41. Ramjaun AR, Tomlinson S, Eddaoudi A, Downward J. Upregulation of two BH3-only proteins, Bmf and Bim, during TGF beta-induced apoptosis. Oncogene 2007;26:970–981
42. Lei K, Davis RJ. JNK phosphorylation of Bim-related members of the Bcl2 family induces Bax-dependent apoptosis. Proc Natl Acad Sci USA 2003; 100:2432–2437